

# Chapter 7

## Pump probe spectroscopy of ultracold Rb<sub>2</sub> molecules

The achievement of cooling an atomic ensemble to temperatures exceeding absolute zero only by less than  $10^{-9}$  K made it possible to investigate atoms in a scope never realizable before [132]. The cooling and trapping of atoms [133, 134] allows for the control over atoms in a regime where the de Broglie wavelength is much larger than the Bohr radius [135]. This new physics is now taking its course towards molecules [136, 137] and new interesting perspectives emerge. The resulting progress leads to a molecular Bose-Einstein Condensate [138, 139, 140], manipulation of molecules [141, 142], an enhanced picture of atom collision physics [50, 143, 144], and ultimately to a molecular laser based on the similar concept of the atom laser [145].

In this chapter attempts of photoassociation of cold Rb<sub>2</sub> molecules by fs pulses and its detection are described. The first sections explain the concept of laser cooling and trapping of atoms. Next, the atomic rubidium is presented in details as a system that is well suited for a Magneto-Optical trap (MOT). Then, photoassociation of atoms is proposed as one of a few possibilities to investigate cold molecules. Afterwards, the experimental setup is demonstrated and finally the results are shown and discussed.

## 7.1 Basics of laser cooling and trapping

The temperature of an ensemble is directly proportional to its random kinetic energy. For this matter the room temperature corresponds to velocities of atoms in a range of a few hundreds of meters per second. In order to cool the atoms down close to absolute zero, they need to be slowed down, and here optical methods become very convenient [146].

In the process of absorption the momentum is transferred from photons to the atoms, and this way, photon recoil is used to slow down the atoms [147, 148, 149]. In such a process the change of velocity is in the order of a few centimeters per second, but given the density of photons, and when exciting a strong atomic transition, it is possible to repeat the process a few million times per second. Since the cooled atoms are traveling at considerable speeds, the frequency of the laser has to be detuned in order to include the Doppler shift [150]. This effect allows for photons to interact with particles traveling towards the laser with a certain speed and slow them down and at the same time be completely transparent for other particles. The arrangement of six laser beams, coming from perpendicular directions, acts upon the atoms as a velocity dependent force. The geometry provides dumping of the atomic motion in any direction and therefore cools the particles. The above presented arrangement is called “optical molasses” [151, 152, 153].

The “optic molasses” method is efficient until the velocities of the atoms are comparable with the photon recoil. The atom which absorbs a photon spontaneously emits one in a random direction after some time and gains momentum. This restraint is called the “Doppler limit” [154] and causes the cooled atoms to diffuse out of the interaction zone, so it does not work well as a trap.

For the trapping of atoms, a mechanism is needed that will pull atoms towards the center of the trap. It can be arranged in various ways. One method is to create a force field with the help of a magnetic field, the strengths of which varies with the position in the trap and is zero at the center of it [48, 155, 156]. This kind of arrangement is realized by an anti Helmholtz configuration of the coils and a proper choice of clockwise and counterclockwise polarization of the cooling laser beams, as presented in Figure 7.1.

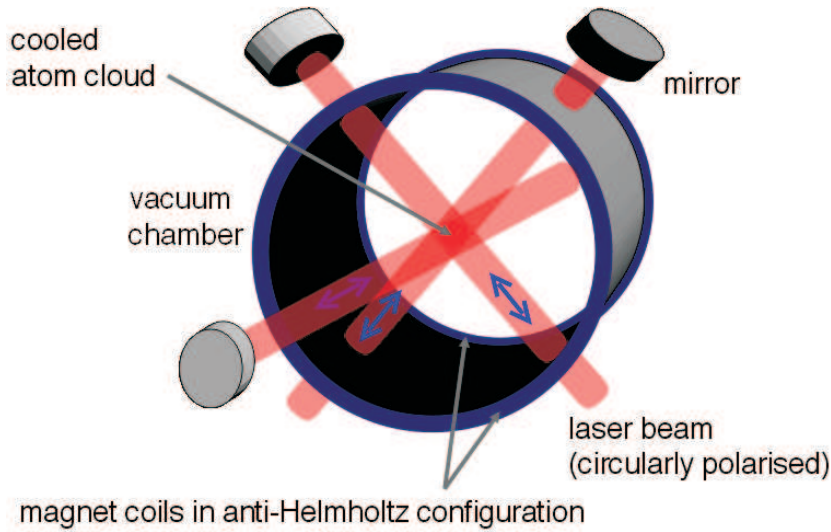


Figure 7.1: Scheme of an Magneto Optical Trap.

The gradient of the magnetic field causes the Zeeman effect to shift the electric levels in atoms, which change their resonance condition. When they move to the outer part of the trap, the energy level shift will lead to absorption of the photons from the properly polarized laser beams. The absorption and the resulting photon recoil can be regarded as an external pressure. A simplified illustration of the mechanism is shown in Figure 7.2. In this way is formed a Magneto-Optical Trap (MOT) also known as Zeeman Optical Trap [146, 157, 158].

## 7.2 Atomic rubidium

Rubidium is a element of group one of the alkali metals, as sodium and potassium. Since it is placed in the first group there is only one electron in the outer shell which can be easily contributed to the ionic bond. The atomic transition structure makes the rubidium a good candidate for trapping and cooling. The basic scheme of cooling is presented in Figure 7.3

The trapping laser is detuned to red roughly 1 to 3 natural linewidths from the  $5S_{1/2}(F=2) \rightarrow 2P_{3/2}(F'=3)$  of  $^{87}\text{Rb}$ . Since about 1/1000 of the population will decay into the  $F=1$  instead of  $F=2$ , the second hyperfine pumping laser is used to pump the population from the  $5S_{1/2}(F=1)$  to  $2P_{3/2}(F'=2)$  from

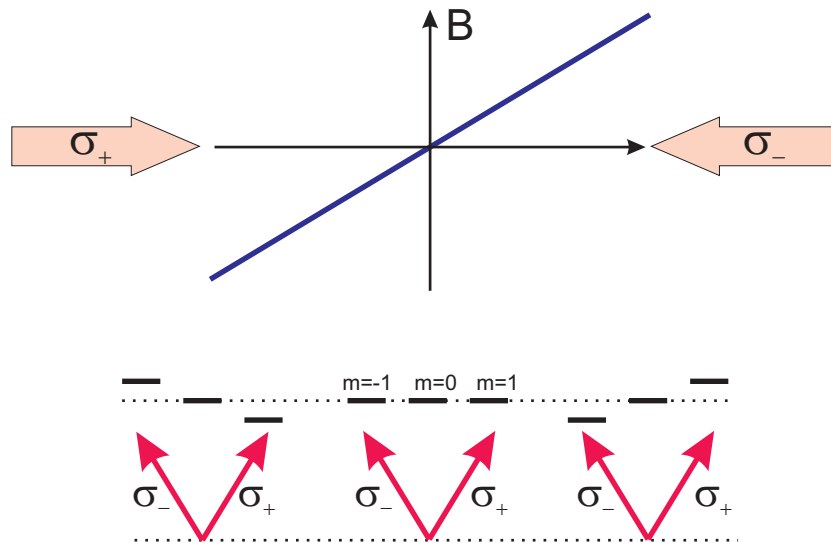


Figure 7.2: Explanation of the MOT. Light polarization coming from opposite directions has an inverse helicity. For this configuration of the lasers the photons coming from the right directions having  $\sigma_-$  polarization will excite only the  $m=-1$  transition whereas for the laser coming from the left having  $\sigma_+$  polarization, the transition  $m=1$  will be affected. Since the laser is detuned from the atomic transition, the absorption takes place for the atoms leaving the zero field point. Effectively, a force field is created that pulls the atoms toward the center of the trap.

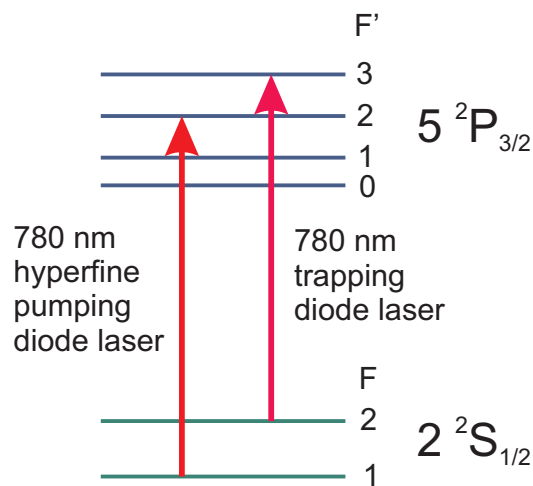


Figure 7.3: Scheme of energy levels of  $^{87}\text{Rb}$  and cooling procedure, including trapping laser and hyperfine pumping laser.

where the population decays to back to the  $F=2$  state and can be further trapped.

In case of a rubidium MOT, the wavelength the of trapping and pumping CW lasers are near 780 nm and therefore diode lasers can be used, which significantly simplifies the laser setup and the frequency stabilization feedback loop.

### 7.3 Photoassociation process

The cooling and trapping techniques applied on atoms are not effective on molecules. Since even the simple diatomic molecules have complex energy potentials it makes them much harder to cool down and almost impossible to trap.

Cooling of molecules is realized by different approaches. Some of them are direct cooling by the use of a buffer gas [159] or by electrostatic slowing [160]. Both of these methods are limited to temperatures not lower than a few mK. The alternative is to use photosynthesis in the Bose-Einstein Condensate via a Feshbach resonance [161, 162] or use the photons to “glue the atoms” together by photoassociation [52, 163].

Photoassociation (PA) of the molecules from cold atoms occupying a MOT creates molecules that are already translationally cold, which avoids the problem of cooling them. The process itself takes place when the two colliding atoms absorb a photon and then become an excited molecule. The excitation normally takes place at distances between the colliding atoms in the order of a few tens of Angstroms, which results in weakly bound excited molecules.

The ground state of the transitionally cold bound molecule can be reached either with CW lasers [52] or alternatively with broad bandwidth pulses [164]. The use of short pulses with a wide spectrum is regarded here as many CW lasers. Additionally, the higher intensities and stronger fields increase the efficiency of the process. Femtosecond pulses also offer many other parameters that can be manipulated, which increases the number of created bond molecules. One of the possible fs-PA scenarios is presented in Figure 7.4. A weak molecular bond is created through resonant excitation

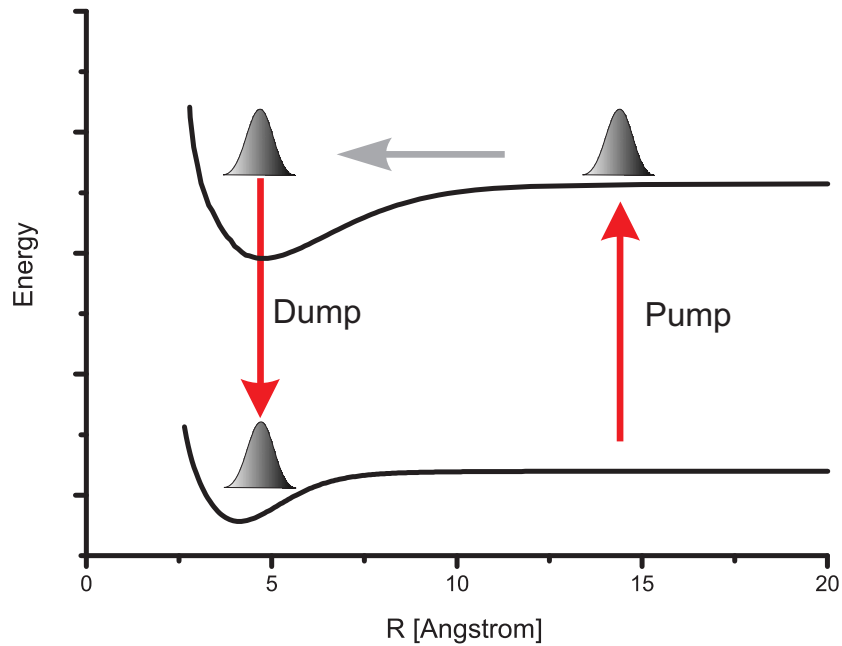


Figure 7.4: One of the simplified scenarios of femtosecond photoassociation.

during the collision. The use of a large bandwidth makes it possible to create a wavepacket traveling inward on the potential where at the proper delay, the population can be dumped to the ground bond state by a second pulse.

## 7.4 Experimental setup

In this experiment, we chose to bond the rubidium atoms by the use of IR laser pulses and detect them by ionization of resulting molecules with the NOPA pulses. The fs pulses were delivered by a RegA seeded by a Mira from Coherent. The system was aligned to work with a repetition rate of 100kHz and at the central frequency 802 nm and the bandwidth of 26 nm.

The pulses, as it is shown in Figure 7.5, are first split by a beamsplitter and 90% of the intensity is directed to pump the NOPA described in the later part of this section, which delivers pulses with their spectrum centered around 496 nm. The remaining 10% are sent through the shaper setup, where the use of 2000 lines/mm gratings together with cylindrical lenses of focal lengths of 250 mm leads to the resolution of 1.3 nm of wavelength

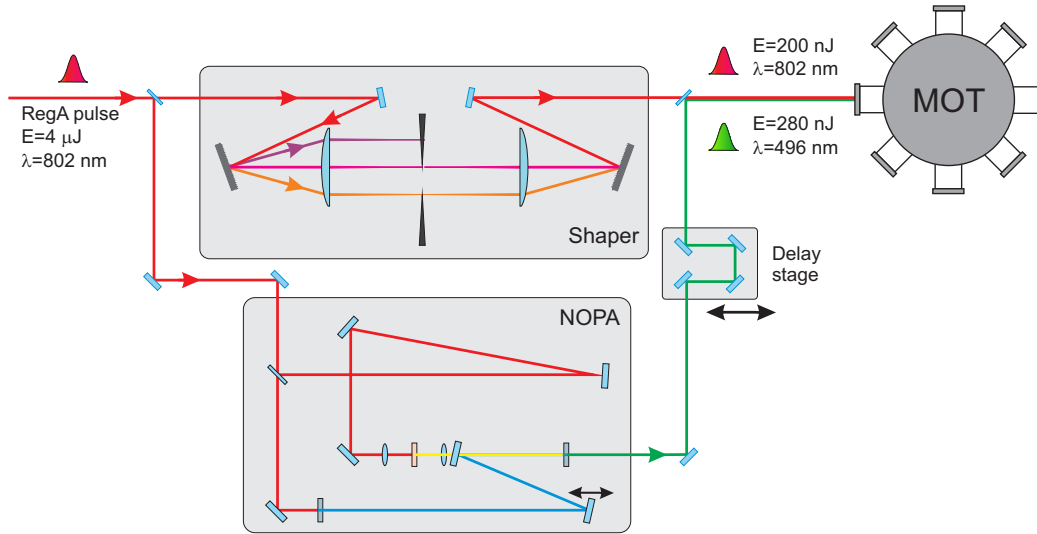


Figure 7.5: MOT experimental setup. For details see text.

change corresponding to a 1 mm translation within the Fourier plane. In this experiment, the control over the transmitted wavelengths from the pulse spectrum is achieved by replacing the modulator by a simple edge attached to an actuator. The edge placement has been chosen in a way that it blocks the blue part of the spectrum from the the  $D_1=795\text{nm}$  line. The purpose of this spectrum modification is necessary, since with this spectral component present the rubidium atoms absorb a macroscopical number of the photons from the fs beam, and the unbalanced recoil blows the trapped ensemble away.

Most of the intensity of the laser is used to pump the NOPA, which was constructed by myself in the frame of this work. The system is based on an already existing 100kHz NOPA built in the Hahn-Meitner Institute in Berlin in cooperation with Prof. Dr. E. Riedle. Originally the first NOPA's were pumped by 1kHz amplified pulses with energies in the range of  $200 \mu\text{J}$  [165, 166]. The energy available from 100kHz RegA amplifiers pumped by a 10 W laser is on the order of a few  $\mu\text{J}$ , therefore significant modifications of the setup have to be made. The details of the construction and the beam geometry can be found in reference [167], so in this thesis only a brief description will be provided.

The NOPA (Noncollinear Optical Parametric Amplifier) [165, 166] is

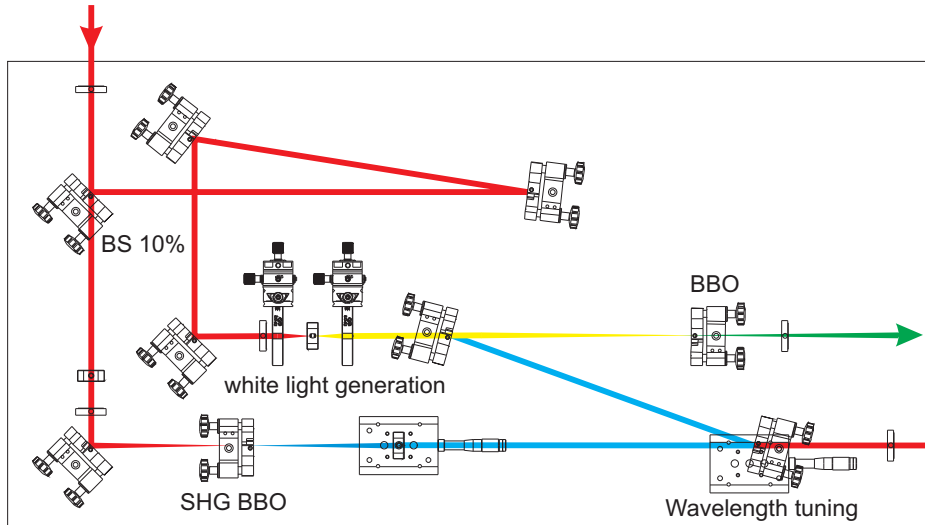


Figure 7.6: NOPA beam and components scheme.

based on parametric amplification of white light that is generated in a sapphire plate [168]. The process takes mainly advantage of self focussing [169, 170] and self phase modulation [171, 172, 173], which are characterized by a high nonlinearity with the intensity of the pulse. Basically, for the white light generation, the intensity threshold has to be reached. For the 1kHz NOPA pumped by few hundred  $\mu\text{J}$ , around 5-6  $\mu\text{J}$  are used to produce the white light, whereas in case of 100kHz lasers, 4-6  $\mu\text{J}$  is the total energy available for pumping. Therefore, first of all, the intensity distribution has to be changed and instead of 5%, 10% of the intensity is used in the white light stage in case of the pump energies at 4  $\mu\text{J}$  or 20% of intensity when pump energies are even lower. Next, to obtain higher intensity at the sapphire crystal, the beam geometry has to be modified. The focusing lenses are exchanged from 50 mm to a focal length of 30 mm, which assures stable generation of white light.

The main part of the pulse intensity is used for a second harmonic generation (SHG). Here, once again we are in disposal of much smaller energies. To achieve similar efficiencies as in a 1kHz NOPA, a doubling crystal is placed in between the telescope lenses, where the optimal intensity for the efficient SHG can be found by changing the position of the crystal along the beam. Later, the second lens of the telescope allows to adapt the size of the beam



waist of the SH beam in the BBO crystal, where the blue pump is temporally and spatially overlapped with the white light. Contrary to the 1kHz NOPA, the BBO crystal is placed directly in the focus of the beam. The layout of the constructed 100kHz NOPA is presented in Figure 7.6.

The homebuild NOPA, when pumped by  $4.5 \mu\text{J}$  at 800nm, delivered as much as 550 nJ at the peak of the tuning curve, which was 510-520 nm. This energy corresponds to an efficiency of the system exceeding 12%, which is quite high for a parametric amplifier. It is also stressed that a stable parametric amplification can be achieved when the NOPA is pumped with energies as low as  $2 \mu\text{J}$ .

The typical tuning range depends from on the pump pulse central frequency, and it is limited from the short wavelengths side by the second harmonic of the pump fundamental frequency. As the NOPA is tuned towards longer wavelengths, the phase distortions in the white light spectrum make it difficult to go near the pump fundamental wavelength. The observed range span from 480 to 620 with the FWHM of the spectra changing from 25 nm, at short wavelengths, to almost 80 nm at the red part, as it is depicted in Figure 7.7. The bandwidth of this particular NOPA for a specific wavelengths could be surely broaden by further improvement of the white light generation and alignment of the the BBO crystal angle.

After crossing the point where the fundamental frequency should be amplified, the amplification of infrared frequencies lower than the fundamental is observed, but due to lack of a spectrometer covering this range it has not been measured in the frame of this work how far these pulses can be tuned.

The outgoing NOPA pulses were not compressed, since for the MOT experiment, too short pulses are not desirable, while the resulting higher intensity will disturb the trap or cause molecular dissociation.

The pulses are sent through a computer controllable delay line, which allows for performing pump and probe scans. Later, with the help of a dichroic mirror, the NOPA beam and the IR pulses modified by the shaper setup, are combined and directed together towards the MOT.

Inside the MOT apparatus the IR and NOPA laser beams are focused on the atomic cloud. The created molecules are recorded by a RF quadrupole as a function of the delay between the NOPA and the IR laser pulses.

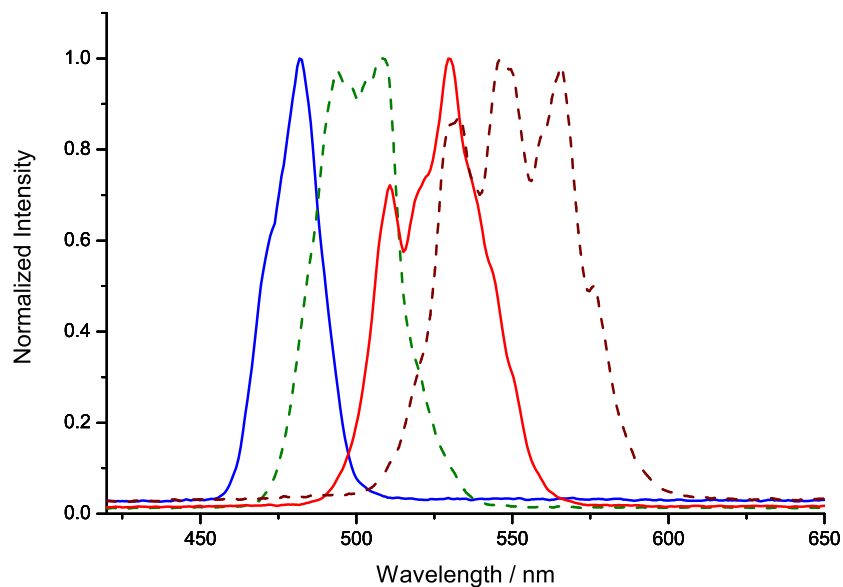


Figure 7.7: Tuning of the NOPA central wavelength.

## 7.5 Results

The pump probe spectrum shown in Figure 7.8 was done with the NOPA and the IR pulses. The following features of the spectrum deserve our attention. First of all, at negative delays, where the NOPA pulse comes first, the rate of detected molecules is on a relative low level, whereas for positive delays an increase in signal is apparent. Next, for positive delays, the signal shows oscillations with a separation between the first two peaks equal to 1.8 ps and for the next ones by 3.3 ps and 3.7 ps, as indicated in Figure 7.8.

The first feature of this spectrum indicates that molecules are prepared with the help of IR pulses, and then ionized later by the NOPA. The later oscillation present at positive delays are believed to be the oscillations of the created wavepacket on the excited state of the bond molecule. Due to the complicated potential structure it is yet not clear if the process takes place through the singlet  $^1\Sigma_g^+$  or triplet  $^3\Sigma_g^+$  state. In any case, the oscillations that are observed are due to wavepacket dynamics in the molecule. In the frame of this thesis, a simplified explanation of the measured signal can be

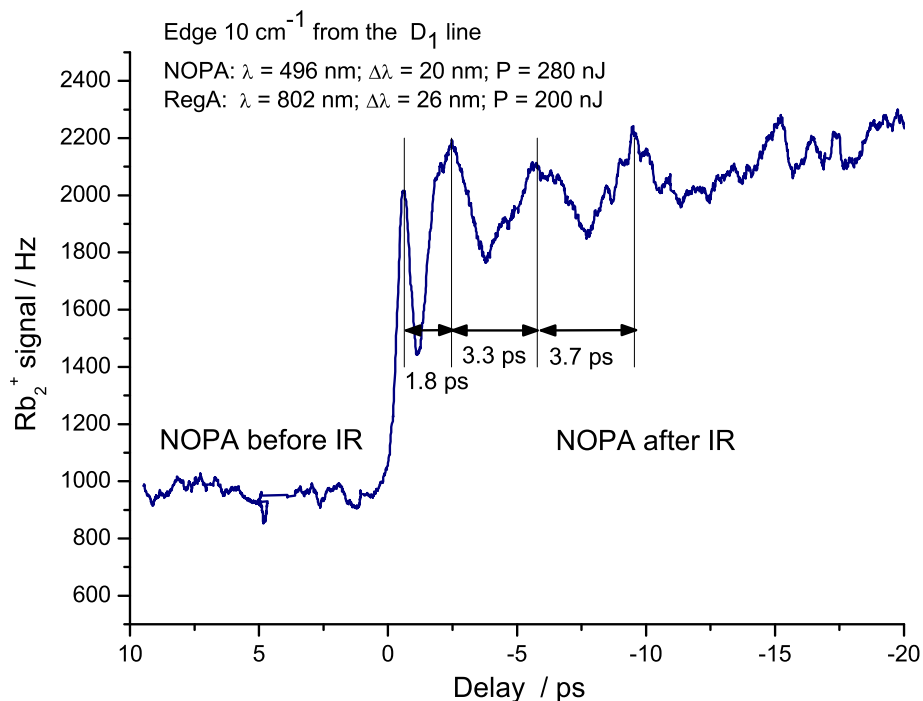


Figure 7.8: Pump probe spectrum of Rb<sub>2</sub> molecule.

given. As it is shown in Figure 7.9, when the IR pulse comes first, it creates weakly bond excited molecules, possibly by photoassociation or by excitation of the molecules already present in the MOT, and at the same time produces a wavepacket which will propagate inwards the molecular potential. At the proper molecular coordinate this population can be detected by ionization. The wavepacket propagates through an optimum position for an ionization on the potential energy surface a few times and this behavior is reflected by the pump probe spectra. The first peak after the crosscorrelation of the pump probe pulses is found at a delay of 1.8 ps, which is when the wavepacket reaches for the first time the inner turning point, where the Franck-Condon factor is favorable for ionization. Then, the next two pronounced peaks are separated by 3.3 ps and 3.7 ps for the oscillating wavepacket. The less pronounced peaks in the spectra at later times could be explained by the

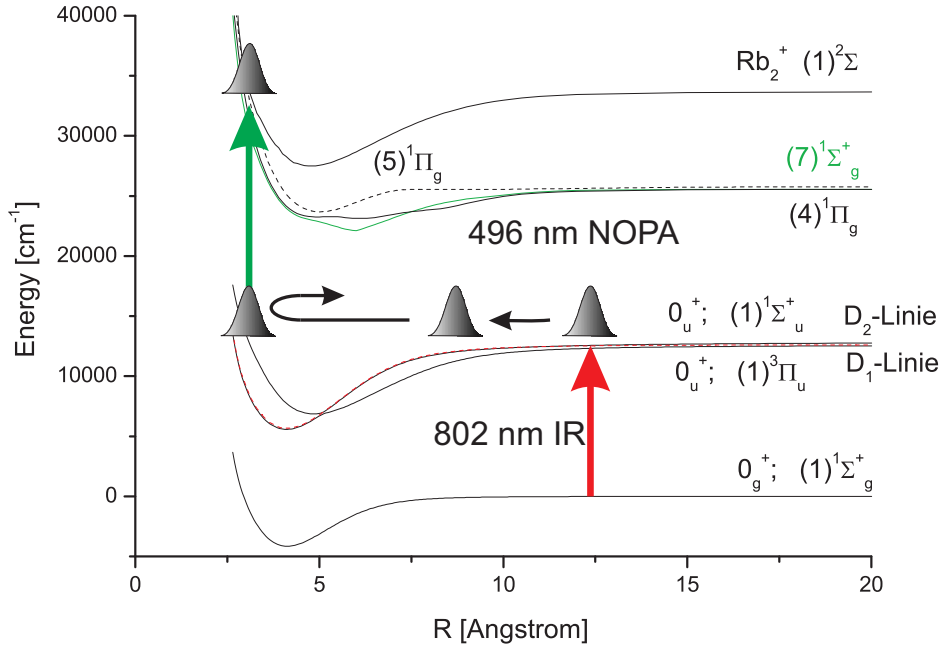


Figure 7.9: Simplified explanation of the observed pump-probe spectrum of  $\text{Rb}_2$  molecules.

dephasing of the propagating wavepacket. Another considered scenario is based on the assumption that the observed wavepacket is created by the a photon process in a energetically higher lying electronic excited state. The verification of this hypothesis would require investigation of the pump probe signal dependency from the intensity of the pump pulses.

A more detailed analysis is needed to understand the observed processes on a deeper level and hopefully it will be presented in the upcoming PhD thesis of Wenzel Salzmann [174] and Franziska Sauer [175].

## 7.6 Summary

In this Chapter the pump probe spectroscopy of ultracold  $\text{Rb}_2$  molecules was presented. The atomic ensemble trapped in the MOT was irradiated by fs pulses with the central wavelength of 802 nm with a modified spectrum, which excluded wavelengths shorter than 795 nm. That allowed for the excitation of colliding molecules in a way that they formed a weak molecular bond. The detection of molecules was realized by ionization, and by 496 nm

central-wavelength pulses provided by a 100kHz NOPA built in the frame of this thesis. The obtained pump and probe spectra show indications of the femtosecond photoassociation process. In order to confirm these findings additional experiments, including a more elaborate control of the wavepacket propagation, for example including a chirp control of the IR pulses and finally closed loop experiments should be performed.

Further perspectives of this research could lead to new fascinating topics like molecular traps, molecular BEC, cold collision physics, and ultimately to a molecular laser.